A STUDY OF SHOCK IMPACTS AND VIBRATION DOSE VALUES ONBOARD HIGH-SPEED MARINE CRAFT

D P Allen, Institute of Sound and Vibration Research, University of Southampton, UK.
D J Taunton, School of Engineering Sciences, University of Southampton, UK.
R Allen, Institute of Sound and Vibration Research, University of Southampton, UK.

SUMMARY

The shocks and impacts encountered on small high-speed craft exceed the limits set for safe working practice according to current standards. European legislation regarding the exposure to vibration will have far reaching effects on the operators of such craft with respect to the safety of their employees. This paper sets out to highlight the vibration dose values that can be expected during typical transits onboard high-speed craft and attempts to clarify some of the controversy currently surrounding vibration dose measurement in such circumstances. In order to relate vibration dosage to the impacts encountered and to boat motion, an algorithm was developed that identifies the timing and magnitude of impacts.

1. INTRODUCTION

Crew and passengers in high-speed craft, such as rigid-hull inflatable boats (RIB), are subjected to a working environment far worse than most other occupations. In addition to the dangers of working at sea, the shocks to the body caused by large magnitude impacts can have severe short-term as well as longer lasting effects on health and well-being. European legislation regarding the exposure of workers to vibration in the workplace [1] will have far-reaching effects for RIB operators and will place the onus firmly on employers to eliminate or at least reduce the exposure of their employees to vibration and shock. A great deal of work is currently being undertaken with this aim in mind. In the case of RIBs, a large amount of effort is being directed, for example, at replacing existing seats with suspension seats that effectively reduce the magnitude of shocks [2]. A more radical approach is being taken by ship designers to improve sea-keeping by altering certain characteristics of hull geometry in an attempt to reduce shocks at source.

In order to assess the potential gains from such improvements, it is necessary to determine if any ensuing reductions in vibration and shock dosage occur. The recommended method for calculating dosages of vibration and shock is based on a fourth power of weighted acceleration signals if crest factors are greater than 6 [3]. There has been some controversy, however, regarding the suitability of this laboratory-derived measure to account for the discomfort felt by passengers and crew onboard RIBs [4]. In particular, it has been argued that vibration dosages calculated in this manner do not emphasise enough the effects of lateral impacts, which, from anecdotal evidence, are thought to be one of the major sources of discomfort.

In this paper, we show that vibration doses based on the fourth power of weighted accelerations are sensitive to the 'roughness' of transits onboard RIBs and that the weighting of individual axes is not required. To achieve this, a number of sea trials were undertaken with a RIB instrumented with tri-axial accelerometers and rate gyros to record shocks and boat motion, respectively. An algorithm was developed to identify the timing of impact events, which enabled estimates to be made of peak magnitudes and changes to boat motion following impacts. Of special interest were the measurements of roll motion following impacts in each of the three translational axes. It is shown that the major contributory factors to changes in roll motion, and by implication to discomfort, result from impacts in all directions and not just from lateral impacts as previously suggested.

The remainder of the paper is organised as follows. Following the introduction, a section on methodology describes the sea trials, data acquisition and signal processing. In particular, we describe the instrumentation, the impact detection algorithm and the method for calculating vibration dose values. In the results section, we first show the vibration dose values obtained for each trial and follow this with analyses of the impact detection algorithm and motion detection. The paper finishes with a discussion of the results and the conclusions drawn.

2. METHOD

2.1 SEA TRIALS

Two trials on the same day approximately three hours apart were undertaken onboard an Atlantic 75 RIB operated by the Royal National Lifeboat Institution (RNLI). The duration of each trial was approximately 90 and 70 minutes, respectively. Both trials contained a mixture of head, beam and following seas. The sea state was estimated to be 3 on the first trial and 2 on the second. Two passengers accompanied an experienced RNLI coxswain on both trials. The average speed in open water during both trials was between 15 knots and 20 knots depending on the direction of travel relative to the waves.

DATA ACQUISITION & SIGNAL PROCESSING

2.2 (a) Instrumentation

The boat was equipped with a tri-axial accelerometer (CFX USCA-TX range ±10 g, 200 Hz mounted resonant frequency) and three rate gyros (Silicon Sensing CRS03-

2, range ±100 deg s^{-1}), which were mounted on a wooden block screwed to the deck towards the bow and not at the centre of gravity of the boat for operational reasons. The axes of the accelerometer were aligned such that the Z axis measured vertical acceleration or heave, the Y axis measured transverse or lateral acceleration and the X axis fore-aft accelerations. The X, Y and Z axes of the rate gyros were aligned to measure roll, pitch and yaw, respectively. The forward positioning of the block on the deck meant that none of the gyros' axes coincided exactly with the boat's centres of roll, pitch and yaw.

Data were recorded using a 16-channel logger (IOTECH Logbook 300) housed in a waterproof and impact resistant case located forward of the coxswain proximal to the transducers. From previous unpublished work the maximum duration of impacts was found to be approximately 100 milliseconds, which suggested a high frequency cut-off of 100 Hz [5]. Therefore, each channel was anti-alias filtered with a second-order Butterworth filter having a cut-off frequency of 100 Hz, sampled at a rate of 250 samples/s and converted to digital format with a 16-bit analogue-to-digital converter. Data from all channels were recorded on a 1-Gbyte flash memory card and processed off-line using MATLAB 7.0.

2.2 (b) Impact Detection

Impact event detection was performed with an algorithm based on Pan and Tompkins' method for heart beat detection from electrocardiograph signals [6]. The main differences between their algorithm and the one described here are that the original was intended to work in real-time and as such used an adaptive threshold while the current algorithm is post-processed with a global threshold and uses two sliding window procedures that firstly eliminate false peaks and secondly determine peak magnitudes. A flowchart of the modified algorithm is shown in Fig. 1 and an example of its application in Fig. 2.

The algorithm is summarised as follows. For a given axis, the de-trended raw acceleration signal is low-pass filtered at 10 Hz with a 4th-order Butterworth filter to give a smoothed acceleration profile. The filtered signal is reversed and filtered again to eliminate phase shifts resulting from the original filtering. The filtered signal is then double differentiated and the absolute value obtained. These two processes accentuate the higher rates of change associated with impacts and suppresses other regions of the signal not associated with impacts. The rectified signal is then smoothed by integration with a 0.1 s, i.e., 25 sample points, sliding window. The integrated signal is further smoothed with a 50^{th}-order moving average filter with a cut-off frequency of ~2 Hz. This additional level of smoothing was not part of the original algorithm of Pan and Tompkins, but is required for this particular application because of the nature of the acceleration signal in which the shape of the impact is dependent on its magnitude. Larger magnitude impacts are characterised by larger rates of onset, i.e., greater slope or attack, whilst lower magnitude impacts have a lower rate of onset. For Pan and Tompkins, this was not a problem since heart beats in general are more uniform in their morphology and the difference between heart beat and artefact is more marked. The addition of the moving average filter effectively results in improved rejection of false events.

Local maxima in the smoothed and integrated signal are found by differentiating the signal and determining the turning points. Inevitably, this method will lead to false peaks being detected, which subsequently require elimination. With this algorithm, false peaks are removed in a twofold process, firstly by selecting only those peaks above a certain threshold, which was found empirically to be 0.015, and secondly by eliminating the peak with the lower magnitude of any consecutive pair of peaks occurring within 200 milliseconds of one another.

Once the locations of the 'true' peaks have been found and event markers defined it is then possible to identify the respective impact magnitudes. The impact magnitudes are defined as the maximum values in 400 millisecond windows centred on the event markers. The windowing process is required because the double differentiation stage identifies points with the highest rate of change of acceleration, which occur immediately before or after peak accelerations, and are by definition offset from the true peaks. Since impacts are typically less than 100 milliseconds in duration and approximately 1 s apart, a window of 400 milliseconds ensures that the likelihood of detecting false maxima is minimised.

The filter used for de-noising the raw acceleration signals was a fourth-order Butterworth type with a cut-off frequency of 80 Hz, i.e., the upper limit of frequency weightings W_d and W_b defined in [3].

In addition to peak acceleration estimation, the event markers were also used to determine boat motions in three axes, i.e., pitch, roll and yaw, at the moment of impacts. Before obtaining the boat motion measures, the rate gyro signals were low-pass filtered to remove noise with a 4^{th}-order Butterworth filter with a cut-off frequency of 10 Hz, reversed and filtered again to remove phase shifts.

2.2 (c) Vibration Dose Values

Vibration Dose Values (VDV) were determined in accordance with BS 6841 [3], i.e., for each axis the VDV was calculated by

$$VDV = \left(\int_0^T a^4(t)dt \right)^{1/4} \quad (1)$$

where T is the duration of the exposure and a is the frequency weighted acceleration. The unit of measure of VDV is $ms^{-1.75}$. The weightings used were W_d for the X and Y axes, and W_b for the Z axis, as defined in [3]. The combined VDV in all axes was determined by

$$VDV_{xyz} = \left(VDV_x^4 + VDV_y^4 + VDV_z^4\right)^{1/4} \quad (2)$$

and the total VDV of both trials by

$$VDV_{TOTAL} = \left(VDV_1^4 + VDV_2^4\right)^{1/4} \quad (3)$$

where VDV_1 and VDV_2 are the combined axis VDVs of trials 1 and 2, respectively, as given by (2).

3. RESULTS

3.1 VDV

Plots of the raw accelerometer signal of each axis recorded during the first trial are shown in Fig. 3. For the first 35 minutes the boat travelled in relatively calm water between its mooring and the harbour entrance. Once in open water the magnitude and frequency of impacts increased significantly. Approximately 82 minutes after the start of the trial, the boat returned to calmer water. Trial 2 followed a similar pattern with the boat in open water for about 40 minutes. During trial 1, the unweighted peak acceleration magnitude for the Z axis was ~8.50 g, while its rms value was ~0.35 g, which resulted in a crest factor, i.e., peak divided by rms, of ~24.3. For trial 2, the maximum was ~5.10 g and rms ~0.24 g, giving a crest factor of ~21.3. These crest factors were well above the threshold of 6 given by [3], above which VDV is deemed to be the correct measure of exposure to whole-body vibration.

VDVs were calculated from the translational accelerations using Eqs.(1-3) and are reported in Table 1a. It can be seen that the total VDV during each trial (48.54 and 25.94 $ms^{-1.75}$) was dominated by the Z axis (48.51 and 25.90 $ms^{-1.75}$) and that the contribution to the VDV from the X axis (4.60 and 1.97 $ms^{-1.75}$) caused by longitudinal impacts was relatively low. It is also apparent from Table 1a that the dose received far exceeded the 15 $ms^{-1.75}$ action limit recommended in BS 6841 [3] and that this limit occurred during trial 1. In Fig. 4 the frequency weighted Z axis acceleration from trial 1 is shown along with a plot of the VDV as a function of time. The time at which the 15 $ms^{-1.75}$ action limit was reached is marked by the vertical dashed line approximately 36 minutes from the beginning of the trial and occurring approximately 2 minutes after the boat had entered rough water. Had trial 2 been the only trial undertaken that day, the time taken to reach the action limit would also have been approximately 2 minutes after entering rough water (not shown). The fact that trial 1 returned higher VDVs in all axes than those for trial 2 was to be expected due to the higher sea state during the first trial.

Since VDV is sensitive to both shocks and vibration, it is interesting to note the estimated contribution to VDV of vibration alone, i.e., without the effects of impacts, and to determine the dosage a person would have received had they been on the boat in calm water with the engine running for the same length of time as the trials. To estimate this, a 2 minute segment of the acceleration signals was identified from the period before the boat reached open water during trial 1. Spectral analysis revealed low frequency components below 2 Hz related to boat motion and higher frequency components in the band between 10-80 Hz caused by general boat vibration, as shown in Fig. 5. By extrapolating a 2 minute segment of each axis to the length of the relevant trial, it was possible to estimate the VDV due to vibration alone for trials 1 and 2. Since the original VDV calculations had been performed on low-pass filtered signals with cut-off frequency 80 Hz and because the boat vibration was above 10 Hz, the acceleration signals were band-pass filtered between 8-80 Hz with a 4^{th}-order Butterworth filter prior to performing the estimation. The estimated VDVs are given in Table 1b. It can be seen that the total VDV due to vibration was estimated to be 2.57 $ms^{-1.75}$ and 2.41 $ms^{-1.75}$ for trials 1 and 2, respectively.

3.2 IMPACT DETECTION

By applying the peak detection algorithm to the unweighted accelerometer signals, it was possible to estimate the timing of impact events and their magnitude for both trials. Table 2 shows the number of impacts from unweighted acceleration signals detected at increasing levels of magnitude for each of the three translational axes.

From the results of the X axis, i.e., longitudinal to the boat, it can be seen that the majority of impacts detected were below 1 g (1001 (97%) and 854 (99%) for trials 1 and 2, respectively) and in fact none were greater than 4 g.

In the case of lateral impacts detected in the Y axis, the majority were also less than 1 g (1415 (85%) and 1681 (95%) for trials 1 and 2, respectively), but, when compared to the X axis, a larger number of impacts above 1 g were also detected (249 and 98). The total number of impacts in the Y axis across both trials (3443) was higher than the total observed in the X axis (1888).

In the case of the Z axis, i.e., vertical impacts, it is noticeably that, in general, impacts at higher magnitudes were more numerous than those encountered in the X and Y axes. The highest valued impact during trial 1 was ~8.5 g, and, in fact, 517 (~23%) of the 2184 total impacts were greater than 2 g. In addition, during trial 1 the number of Z axis impacts in the 0-1 g band was similar to that for the 1-2g band (857 and 810, respectively) in contrast to the X and Y axes in which the majority of impacts were below 1 g.

During trial 2 the sea state was lower than the first trial and the number of higher valued impacts was reduced accordingly. Less than 5% of the 2181 total impacts were above 2 g, and the majority (1601 or 73%) were below 1 g.

The relative numbers and magnitudes of impacts in the Z axis across both trials correspond with the dominance of the Z axis to the total VDVs, as noted in Table 1a. The total number of impacts received in each axis during both trials was similar, but because of the different sea states, and hence magnitude of

accelerations, the VDV of trial 1 (48.5 $ms^{-1.75}$) was much greater than that of trial 2 (25.9 $ms^{-1.75}$).

3.3 MOTION DETECTION

In addition to determining peak acceleration magnitudes, the event markers were also used to determine changes in boat motion, i.e., pitch, roll and yaw, in response to impacts. Using such a scheme it was possible to determine the number of occasions that the impacts reported in Table 2 caused a change in motion greater than some pre-determined threshold. In Tables 3 and 4 the number of occasions that the change in boat motion exceeded a pre-defined threshold of 10 deg s^{-1} following impacts is reported for trial 1 and 2, respectively. The tables list the number of changes to the roll, pitch and yaw greater than the threshold resulting from impacts in each of the three translational axes at increasing acceleration magnitudes. Motion changes were calculated by finding the absolute difference between the mean motion before and after an impact. The mean motions were defined as the average motions from 100 ms windows, i.e., 25 samples, before and after the impacts. The size of this window was chosen to reflect the typical duration of impacts.

From Table 3 it can be seen that during trial 1, longitudinal impacts in the X axis caused a total of 313 changes greater than 10 deg s^{-1} to the boat's roll from a total of 1032 impacts (from Table 2), 128 changes to pitch and 0 to yaw. In the Y axis these totals increased to 704, 485 and 6, respectively, from a total of 1664 impacts. In the Z axis, there were 1191 changes to roll, 479 to pitch and 6 to yaw from a total of 2184 impacts.

For all axes, the proportion of total impacts above 1 g that caused changes in motion was higher than that of impacts below 1 g. For example, in the case of the Z axis, the number of changes to the roll (X axis) resulting from impacts between 0-1 g was 117 out of a total of 857 such impacts, i.e., ~14% of the total (from Table 2), whereas for the 1-2 g band there were 616 changes from 810 impacts or 76% of the total, and 260 from 298 (87%) in the 2-3 g band. These results corresponded with expectations since the higher the magnitude of impact, the greater the likelihood of causing a change in motion above the threshold.

The same pattern of results from trial 1 also occurred during trial 2 in that the number of changes to roll was higher than that of pitch, which in turn was higher than the yaw. In fact, no changes in yaw above the threshold were detected during trial 2. For Z axis impacts, the proportion of impacts causing changes above the threshold was 86 from 1601 impacts in the 0-1 g band (~5%), 327 from 476 in the 1-2 g band (~69%), and 73 from 84 in the 2-3 g band (~87%). It can be seen from the tables that, in general, as the impact magnitude increased, the probability of inducing a change in motion above the threshold increased accordingly.

If the proportions of total changes in roll are considered, then for X axis impacts 313 changes in roll motion occurred from a total of 1032 impacts during trial 1 (~30%) and 50 changes from 856 impacts (~6%) during trial 2.

Impacts in the Y axis caused 704 changes in roll from 1664 impacts (~42%) during trial 1 and 333 changes from 1779 impacts in trial 2 (~19%).

In the Z axis, the number of changes in roll during trial 1 was 1191 from 2184 impacts (~55%) and 504 changes from 2181 impacts (~23%) during trial 2.

4. DISCUSSION

The total VDV of 49.5 $ms^{-1.75}$ experienced by the crew during the trials far exceeded the action limit of 15 $ms^{-1.75}$ recommended in BS 6841 [3] and the maximum daily dose of 21 $ms^{-1.75}$ permitted by the European Directive [1]. That the action limit was reached after only 2 minutes of the first trial in relatively rough water is particular concerning, especially when considering the adverse long-term health effects experienced by RIB crew and passengers [7] who frequently spend longer periods at sea often in worse conditions than those reported here. The higher VDV of the first trial in comparison to that of the second was to be expected given the increased sea state during the former.

It is also interesting to note that the total VDVs were dominated by the VDV of the Z axis and that the impacts in the Y axis had little effect on the VDV despite the relative importance suggested by anecdotal evidence that lateral impacts have on discomfort. This would appear to support the argument that, although it is generally held to be a measure of discomfort, based on translational accelerations alone, VDV does not adequately represent the level of discomfort reported onboard high-speed craft. However, the differences between the actual VDVs calculated for the two trials (48.54 $ms^{-1.75}$ and 25.94 $ms^{-1.75}$) and those estimated to be due to vibration alone (2.57 $ms^{-1.75}$ and 2.41 $ms^{-1.75}$) are large enough to suggest that, irrespective of the axis, the presence of high magnitude impacts in rough seas has a significant effect on the VDV obtained.

If the changes to boat motions due to impacts are considered, then it can be seen that the changes in roll motion occur irrespective of the axis in which the impact occurred. This can be explained by the fact that the boat does not generally impact perpendicular to the sea surface and as a result will tend to roll on impact. The rougher the sea, the more apparent this effect becomes and the greater the degree of roll. During trial 1, 30% of impacts in the X axis resulted in a change in roll greater than 10 deg s^{-1}, 42% of impacts in the Y axis produced a similar change in roll as did 55% of impacts in the Z axis. During trial 2, in which the magnitudes of impacts were generally lower due to the lower sea state, these figures were reduced to 6%, 19% and 23% for the X, Y and Z axis, respectively.

As stated in the Introduction, anecdotal evidence suggests that the major source of discomfort encountered onboard RIBs is from lateral impacts. This present work, however, suggests that it is not lateral impacts *per se* that are the major source of movement-induced discomfort.

Rather, the problem is caused by the roll following impacts in any of the three axes . In fact, it was shown that impacts in the Z axis contribute more to the boat's roll than do the lateral Y axis impacts. Therefore, if VDV alone is not considered adequate to measure discomfort onboard high-speed craft, then, instead of weighting the Y axis accelerations more than other axes as has been suggested [4], it might be more appropriate to include the amount of roll with the VDV. It might also prove useful to include the number of impacts encountered and their magnitude in a multivariate analysis to obtain any such measure.

5. CONCLUSIONS

This paper has highlighted the vibration dose values that can be expected onboard high-speed marine craft and how these values relate to limits set by current standards and legislation. By comparing the impacts encountered to the boat motions, it has been possible to determine which are the more dominant axes and show that it is not necessary to weight certain axes more than others.

In further work we intend to repeat these experiments in higher sea states and with different boats. The magnitudes of impacts reported in this work are lower than those in other work [4]. However, it is not clear how their data were collected and analysed, and therefore it is not easy to gauge the accuracy of their results. It is reasonable to assume though that the impacts encountered would have been larger due to the higher sea states.

It is also intended to apply the algorithms and analysis reported here to a series of model tank test experiments involving a variety of hull forms. From these experiments it should be possible to determine each hull's VDV and motion characteristics in a variety of sea conditions, which could prove useful to naval architects designing RIBs that exhibit better performance regarding the new legislation.

6. REFERENCES

[1] European Council, "Directive 2002/44/EC of the European Parliament and of the Council of 25 June 2002 on the minimum health and safety requirements regarding the exposure of workers to the risks arising from physical agents (vibration)," *Official Journal of the European Communities*, vol. L 177, pp. 13-19, July2002.

[2] C. M. Barnard and J. L. van Niekerk, "Suspension seat for high speed off-shore rigid inflatable boats," *41st United Kingdom Group Meeting on Human Responses to Vibration, QinetiQ, Farnborough, UK*, 2006.

[3] British Standards Institute, "BS 6841: Measurement and evaluation of human exposure to whole-body mechanical vibration and repeated shock,"1987.

[4] T. Dobbins, S. Myers, and J. Hill, "Multi-axis shocks during high speed marine craft transits," *41st United Kingdom Group Meeting on Human Responses to Vibration, QinetiQ, Farnborough, UK*, 2006.

[5] J. T. Broch, *Mechanical Vibration and Shock Measurements* Bruel & Kjaer, 1980.

[6] J. Pan and W. J. Tompkins, "A Real-Time QRS Detection Algorithm," *IEEE Transactions on Biomedical Engineering*, vol. 32, no. 3, pp. 230-236, 1985.

[7] W. Ensign, J.A. Hodgdon, W.K. Prusaczyk, D. Shapiro and M. Lipton, "A Survey of Self-Reported injuries Among Special Boat Operators," *Naval Health Research Center*, Report No. 00-48, pp. 1-19, 2000.

VDV	Trial 1	Trial 2	Total
X-axis	4.60	1.97	4.64
Y-axis	10.54	7.33	11.11
Z-axis	48.51	25.90	49.47
Total	48.54	25.94	49.50

Table 1a. VDV in each axis and totals for both trials

VDV	Trial 1	Trial 2	Total
X-axis	0.13	0.12	0.14
Y-axis	1.26	1.19	1.46
Z-axis	2.53	2.37	2.92
Total	2.57	2.41	2.96

Table 1b. Projected VDV in each axis and totals for both trials due to boat vibration excluding impacts

Acc. Mag.	X-axis (Longitudinal)			Y-axis (Lateral)			Z-axis (Vertical)		
	Trial 1	**Trial 2**	**Total**	**Trial 1**	**Trial 2**	**Total**	**Trial 1**	**Trial 2**	**Total**
0-1 g	1001	854	1855	1415	1681	3096	857	1601	2458
1-2 g	28	2	30	208	89	297	810	476	1286
2-3 g	2	0	2	36	9	45	298	84	382
3-4 g	1	0	1	4	0	4	119	18	137
4-5 g	0	0	0	1	0	1	53	1	54
5-6 g	0	0	0	0	0	0	28	1	29
6-7 g	0	0	0	0	0	0	13	0	13
7-8 g	0	0	0	0	0	0	4	0	4
8-9 g	0	0	0	0	0	0	2	0	2
>9g	0	0	0	0	0	0	0	0	0
Total	1032	856	1888	1664	1779	3443	2184	2181	4365

Table 2. Breakdown of impact magnitudes detected in 3-axes from unweighted accelerations during both trials.

Acc. Mag.	X-axis Impacts			Y-axis Impacts			Z-axis Impacts		
	X-axis motion	**Y-axis motion**	**Z-axis motion**	**X-axis motion**	**Y-axis motion**	**Z-axis motion**	**X-axis motion**	**Y-axis motion**	**Z-axis motion**
0-1 g	293	117	0	489	286	0	117	66	0
1-2 g	17	11	0	178	160	3	616	200	2
2-3 g	2	0	0	33	34	3	260	103	3
3-4 g	1	0	0	4	4	0	108	54	0
4-5 g	0	0	0	0	1	0	48	25	1
5-6 g	0	0	0	0	0	0	25	17	0
6-7 g	0	0	0	0	0	0	12	8	0
7-8 g	0	0	0	0	0	0	3	4	0
8-9 g	0	0	0	0	0	0	2	2	0
>9g	0	0	0	0	0	0	0	0	0
Total	313	128	0	704	485	6	1191	479	6

Table 3. Total changes in motion > 10 deg/s following impacts in the X, Y and Z axes (roll, pitch and yaw) at increasing acceleration magnitude during trial 1.

Acc. Mag.	X-axis Impacts			Y-axis Impacts			Z-axis Impacts		
	X-axis motion	**Y-axis motion**	**Z-axis motion**	**X-axis motion**	**Y-axis motion**	**Z-axis motion**	**X-axis motion**	**Y-axis motion**	**Z-axis motion**
0-1 g	49	25	0	261	152	0	86	81	0
1-2 g	1	0	0	66	59	0	327	75	0
2-3 g	0	0	0	6	5	0	73	30	0
3-4 g	0	0	0	0	0	0	16	6	0
4-5 g	0	0	0	0	0	0	1	0	0
5-6 g	0	0	0	0	0	0	1	0	0
6-7 g	0	0	0	0	0	0	0	0	0
7-8 g	0	0	0	0	0	0	0	0	0
8-9 g	0	0	0	0	0	0	0	0	0
>9g	0	0	0	0	0	0	0	0	0
Total	50	25	0	333	216	0	504	192	0

Table 4. Total changes in motion > 10 deg/s following impacts in the X, Y and Z axes (roll, pitch and yaw) at increasing acceleration magnitude during trial 2.

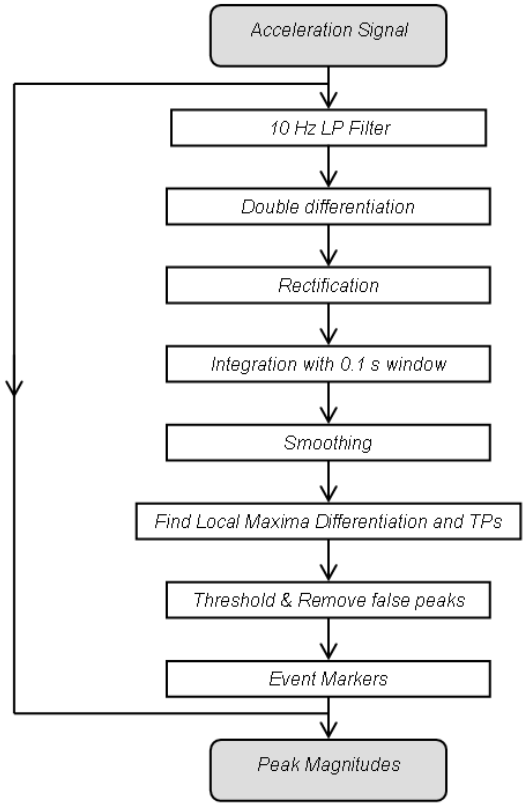

Figure 1. Flowchart showing the main stages of the peak detection algorithm beginning with the acceleration time series and terminating with a set of peak magnitudes and event markers, which are also used to determine boat motions.

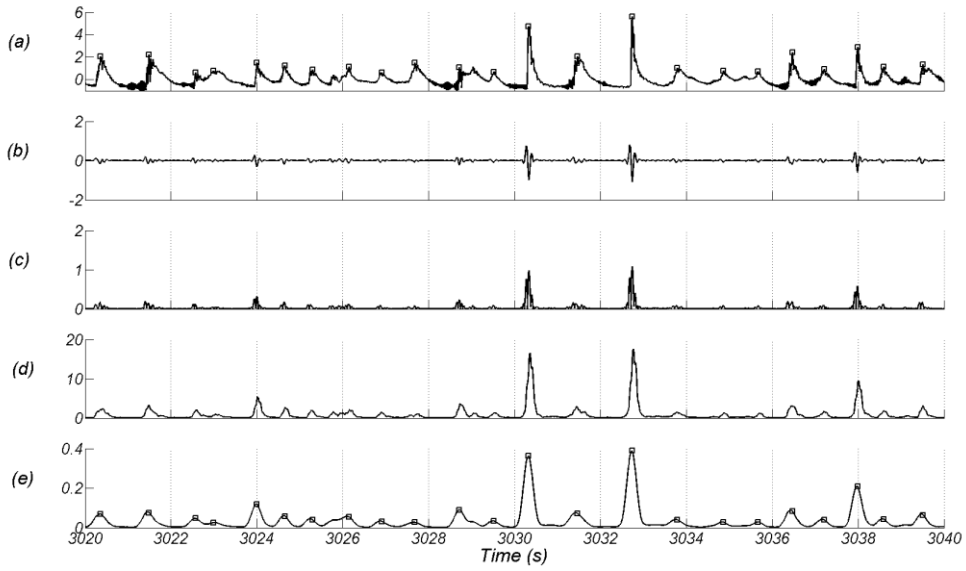

Figure 2. Plots of the various stages of the impact event detection algorithm applied to a 20 s segment from the Z axis acceleration time series obtained during trial 1. (a) shows the original acceleration signal. Also included in this plot are the peak magnitudes as detected by the algorithm shown by the square markers. (b) shows the result of double differentiating the filtered acceleration time series and (c) shows the absolute or magnitude of this signal. (d) shows the integrated squared signal and in (e) this signal is further smoothed with a LP filter to eradicate false peaks. The same event markers from the first plot superimposed are also shown in (e).

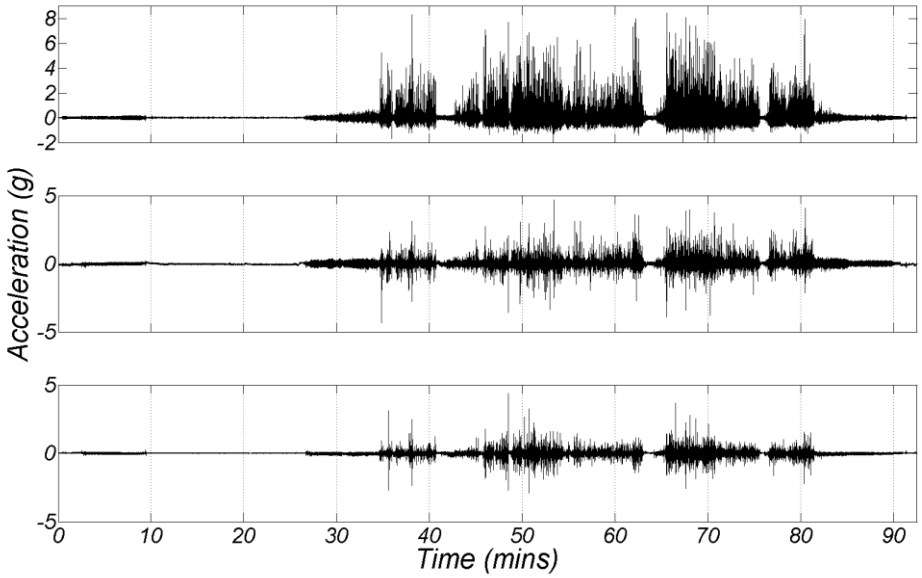

Figure 3. Plots of unweighted and unfiltered accelerations from the first trial. (Top, Z axis; middle, Y axis; bottom, X axis).

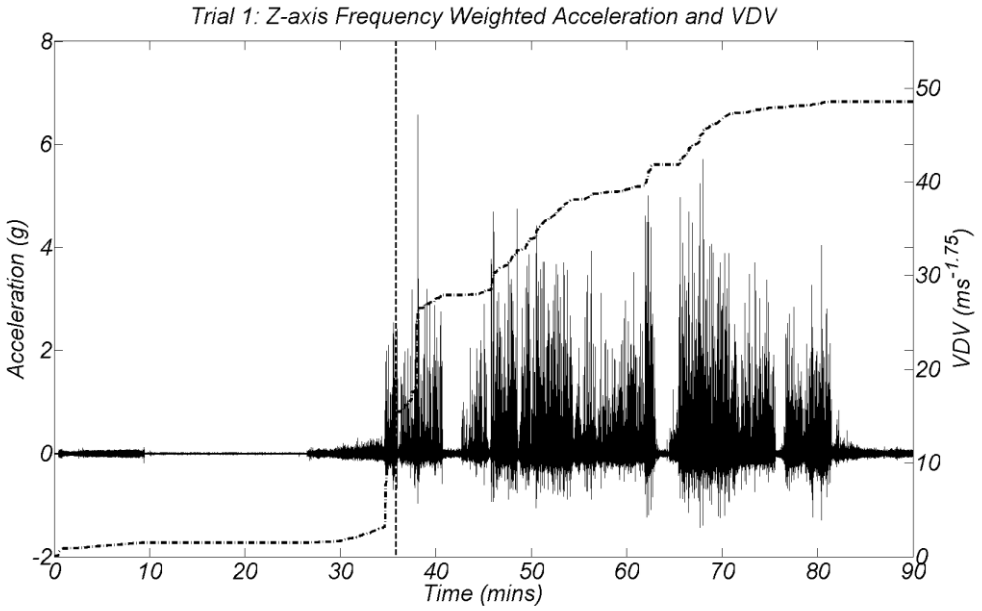

Figure 4. Plots of Z axis frequency weighted acceleration (solid line) and VDV as a function of time (dotted line) from trial 1. The vertical dashed line indicates the time at which the dose action limit of 15 $ms^{-1.75}$ was reached.

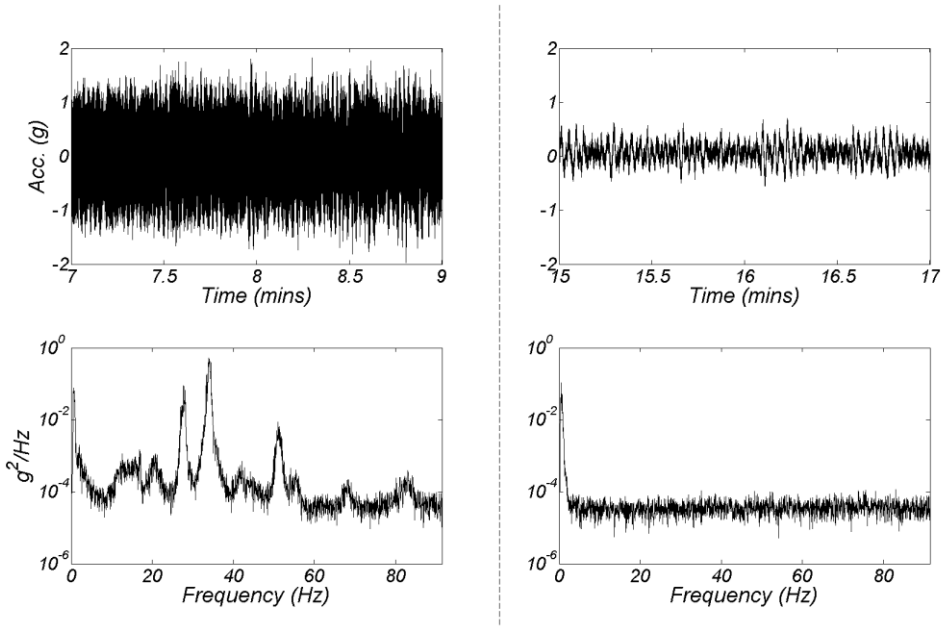

Figure 5. Plots showing the difference in spectral content of acceleration time-series obtained with (a) and without (b) the boat's engine running. The time series (top plots) are 2-minute segments of the Z axis accelerometer signal from trial 1, see Fig. 3. From the power spectra of these signals (lower plots), it can be seen that there is a common peak below ~2 Hz caused by the motion of the boat. The peaks above ~10 Hz observed in the spectrum in (a) are due to engine vibration.